

The local potential approximation for the Brueckner G -matrix and a simple model of the scalar-isoscalar Landau-Migdal amplitude

 M. Baldo^{1,a}, U. Lombardo^{2,3}, E.E. Saperstein⁴, and M.V. Zverev⁴
¹ INFN, Sezione di Catania, 57 Corso Italia, I-95129 Catania, Italy

² INFN-LNS, 44 Via S. Sofia, I-95123 Catania, Italy

³ Dipartimento di Fisica, 57 Corso Italia, I-95129 Catania, Italy

⁴ Kurchatov Institute, 123182, Moscow, Russia

Received: 2 November 2001

Communicated by P. Schuck

Abstract. The Brueckner G -matrix for a slab of nuclear matter is analyzed in the singlet 1S and triplet $^3S+^3D$ channels. The complete Hilbert space is split into two domains, the model subspace S_0 , in which the two-particle propagator is calculated explicitly, and the complementary one, S' , in which the local potential approximation is used. This kind of local approximation was previously found to be quite accurate for the 1S pairing problem. A set of model spaces $S_0(E_0)$ with different values of the energy E_0 is considered, E_0 being the upper limit for the single-particle energies of the states belonging to S_0 . The independence of the G -matrix on E_0 is assumed as a criterion for the validity of the local potential approximation. It turns out that such an independence holds within few percents for $E_0 = 10$ – 20 MeV, for both channels under consideration. The G -matrix within the local potential approximation is used for justifying a simple microscopic model for the coordinate-dependent scalar-isoscalar component $f(r)$ of the Landau-Migdal amplitude in terms of the free T -matrix.

PACS. 21.30.Fe Forces in hadronic systems and effective interactions – 21.65.+f Nuclear matter – 21.60.-n Nuclear-structure models and methods

1 Introduction

The most reliable predictions of nuclear properties come from phenomenological approaches including the macroscopic-microscopic method [1–3], and, at a more fundamental level, the finite Fermi systems (FFS) theory [4–6], the HF method with effective forces [7,8] and the new versions of the energy functional method [9]. These methods, being comparatively simple, permit to carry out systematic calculations for atomic nuclei. On the other hand, being phenomenological, these approaches need a set of adjustable parameters. This point appears especially delicate when one is dealing with new types of nuclear systems, *e.g.*, nuclei in the drip line vicinity. Indeed, any extrapolation of phenomenological parameters found for stable nuclei is hardly reliable in this case. Therefore the old problem of the *ab initio* calculation of these parameters is of importance not only from a heuristic point of view but also from the practical one. In this paper, we present a rather simple and powerful tool for the development of a nuclear theory starting from a free NN interaction. We give also an example of the application of this method

by constructing a realistic semi-microscopic model for the scalar-isoscalar Landau-Migdal amplitude.

In the application of the microscopic theory of nuclear matter to finite nuclei (see, *e.g.*, the monographs [10] and [11]) the main restriction is the so-called local density approximation (LDA). The LDA works reasonably well inside a nucleus but fails at the surface where there is a domain of density values for which nuclear matter is unstable. However, it is impossible to develop a self-consistent nuclear theory without any consistent description of the nuclear surface. Indeed, just in the surface region the nuclear mean field sharply changes from zero outside the nucleus to a constant value inside. In terms of the FFS theory, this is associated with a sharp variation of the scalar-isoscalar Landau-Migdal amplitude f from a strongly negative (attractive) value outside the nucleus to almost zero inside. A consistent description of this variation is of primary importance for nuclear theory. We intend to develop an approach to this problem based on the Brueckner theory for nonuniform systems beyond LDA.

Recently [12], dealing with 1S -pairing problem for semi-infinite nuclear matter, we developed a method of solving the Bethe-Goldstone (BG) equation with a

^a e-mail: baldo@ct.infn.it

separable form of the Paris NN potential without using any local approximation. The same method was applied to the case of the slab geometry in refs. [13,14]. Though the separable form of the NN interaction simplifies calculations significantly, they remain to be rather cumbersome and much CPU time consuming. To circumvent this difficulty, we devised a new version of the local approximation, that was implemented for the study of the effective pairing interaction $\mathcal{V}_{\text{eff}}^{\text{p}}$ [12]. To distinguish it from the standard LDA, we named it as the local potential approximation (LPA). The effective interaction is associated with the splitting of the complete Hilbert space S into two domains. The first one is the model subspace S_0 , in which the gap equation is written down in terms of the effective interaction $\mathcal{V}_{\text{eff}}^{\text{p}}$. The second one is the complementary subspace S' , in which the equation for $\mathcal{V}_{\text{eff}}^{\text{p}}$ is obtained in terms of the free NN interaction \mathcal{V} . In this subspace, the pairing effects are not significant, therefore the equation for $\mathcal{V}_{\text{eff}}^{\text{p}}$ has the form of the BG equation. Dealing with the pairing problem, the model space was taken in a form convenient for nuclear application, which includes all the single-particle states with negative energies ε_λ . The LPA is related to the calculation of the two-particle propagator in the complementary space which enters the equation for $\mathcal{V}_{\text{eff}}^{\text{p}}$. Roughly speaking, the LPA procedure consists in replacing the exact BG propagator by a suitable form taken from infinite nuclear matter. For a fixed value of the average centre-of-mass (CM) x -coordinate $X = (X_{12} + X_{34})$ of incoming and outgoing nucleons (the x -axis is perpendicular to the layer), the propagator is supposed to be equal to the one of nuclear matter in the potential well $V(X)$. Such an approximation turned out to be accurate at a level of a few percent even at the surface [12]. This was shown by a comparison of the direct solution for $\mathcal{V}_{\text{eff}}^{\text{p}}$ with the LPA one.

From the computational point of view, the problem of finding the Landau-Migdal interaction amplitude in terms of the Brueckner G -matrix is much more complicated than the pairing problem. First, the additional triplet 3S -channel (coupled with the 3D one) should be considered for which the calculations turned out to be more complicated than those for the singlet 1S -channel. Second, instead of fixing the value of the total perpendicular momentum $P_\perp = 0$ as in the pairing problem, the integral over P_\perp occurs in this case. Though the direct numerical solution of the problem, in principle, is possible [15], it looks very difficult. Therefore it is natural to attempt to use LPA for solving the BG equation for the G -matrix that significantly simplifies the calculations. In the case of the singlet 1S -channel, the accuracy of LPA for the BG equation is just the same as in the pairing problem because the corresponding two-particle propagators in the complementary space are the same. As to the triplet channel, applicability of the LPA is not obvious at all. The main goal of this paper is to clarify the latter point.

In the case of the BG equation, there is no evident gain in introducing the effective interaction and it seems more reasonable, after splitting the Hilbert space as $S = S_0 + S'$, to formulate the LPA procedure in a direct way. Accord-

ing to that splitting, the two-particle propagator A in the BG equation can be written as the sum of $A = A_0 + A'$. The model space term, A_0 , should be calculated exactly, whereas the second one, A' , within LPA. It is clear that the applicability of the LPA depends on the choice of the model space S_0 . Indeed, all the quantum and finite-range effects originate mainly from the states nearby the Fermi surface whose contribution to the BG equation is strengthened by the small values of the energy denominator in the two-particle propagator. These contributions produce the long-range components of A and should be taken into account exactly. At the same time, the individual contribution of a far-lying state is negligible and only the sum of a huge number of such states is important. They produce the short-range term of A and can be considered within the local approximation. Hence, the accuracy of LPA should depend on the choice of the model space: the wider is S_0 , the more accurate it is. We use this simple physical idea to impose a criterion of the applicability of LPA. We define the model space $S_0(E_0)$ including all the single-particle states with the energies $\varepsilon_\lambda < E_0$ which is more general than that for the pairing problem¹. It is obvious that a larger E_0 corresponds to a higher accuracy of the LPA. We consider the LPA to be valid at some value of E_0 if the G -matrix does not practically change with additional increase of E_0 .

The paper is organized as follows. Section 2 contains the BG equation for the slab of nuclear matter with separable NN forces. In sect. 3 the splitting of the Hilbert space in the model subspace defined by the cut-off energy E_0 and its complementary subspace is discussed. In addition, the LPA for the BG equation is introduced. In sect. 4 the validity of the LPA for the calculation of the G -matrix in the singlet 1S -channel is analyzed for different values of E_0 . In sect. 5 the analysis is extended to the triplet $^3S + ^3D$ channel. In sect. 6 the G -matrix obtained within LPA is used to justify a simple microscopic model for the scalar-isoscalar component $f(r)$ of the Landau-Migdal amplitude in terms of the off-shell free T -matrix suggested recently [16]. Section 7 contains a summary of the results.

2 Bethe-Goldstone equation for the slab system

Let us consider the BG equation for the G -matrix of two nucleons at the Fermi surface, *i.e.* with the single-particle energies $\varepsilon_\lambda = \mu$, where μ is the chemical potential of the system under consideration. In a short notation it reads:

$$G(E) = \mathcal{V} + \mathcal{V}A(E)G(E), \quad (1)$$

where \mathcal{V} is the free NN potential, $E = 2\mu$, and A is the two-particle propagator which is determined by the integration over the relative energy of the product $(\mathcal{G}^p \mathcal{G}^p)$ of two *particle* single-particle Green's functions. The contribution $(\mathcal{G}^h \mathcal{G}^h)$ of two *holes* is neglected.

¹ The latter corresponds to $E_0 = 0$.

To speed up the convergence it is convenient to renormalize eq. (1) in terms of the free off-shell T -matrix taken at negative energy $E = 2\mu$. The latter obeys the Lippman-Schwinger equation:

$$T(E) = \mathcal{V} + \mathcal{V}A^{\text{fr}}(E)T(E), \quad (2)$$

where $A^{\text{fr}}(E)$ is the propagator of two free nucleons with the total energy E .

The renormalized BG equation has the form:

$$G = T + T(A - A^{\text{fr}})G. \quad (3)$$

We consider a nuclear-matter slab of thickness $2L$ placed into the one-dimensional Saxon-Woods potential $V(x)$ symmetrical with respect to the point $x = 0$ with depth of $V_0 = 50$ MeV, the diffuseness parameter $d = 0.65$ fm, and $L = 8$ fm.

We use the separable version [17,18] of the Paris NN potential [19] which for the 1S_0 -channel has the 3×3 form:

$$\mathcal{V}(\mathbf{k}, \mathbf{k}') = \sum_{ij} \lambda_{ij} g_i(k^2) g_j(k'^2). \quad (4)$$

For the triplet $^3S_1 + ^3D_1$ channel, a similar 4×4 expansion (4) is valid with a formal substitution $g_i(k^2) \rightarrow \hat{g}_i(k^2)$, where the column \hat{g}_i contains two components:

$$\hat{g}_i(k^2) = \begin{pmatrix} g_i^{L=0}(k^2) \\ g_i^{L=2}(k^2) \end{pmatrix}, \quad (5)$$

L being the relative orbital momentum in the CM system.

The scheme of solving the BG equation for a slab of nuclear matter in the mixed coordinate-momentum representation, which has been devised in ref. [15], is adopted also here. Therefore we write down in the explicit form only those equations which are necessary for understanding the procedure and refer to ref. [15] for details. We consider first the singlet channel $S = 0$. As it was mentioned above, all relations remain valid for the triplet channel as well after replacing $g_i(k^2) \rightarrow \hat{g}_i(k^2)$.

The separable form (4) of the NN potential in eqs. (1) and (2) induces similar expansions for the G -matrix

$$G(k_{\perp}^2, k'_{\perp}{}^2, \mathbf{P}_{\perp}; x_1, x_2, x_3, x_4; E) = \sum_{ij} G_{ij}(X, X'; E, \mathbf{P}_{\perp}) g_i(k_{\perp}^2, x) g_j(k'_{\perp}{}^2, x'), \quad (6)$$

and T -matrix

$$T(k_{\perp}^2, k'_{\perp}{}^2, \mathbf{P}_{\perp}; x_1, x_2, x_3, x_4; E) = \sum_{ij} T_{ij}(X - X'; E, \mathbf{P}_{\perp}) g_i(k_{\perp}^2, x) g_j(k'_{\perp}{}^2, x'). \quad (7)$$

Here the form factors $g_i(k_{\perp}^2, x)$ in the mixed representation are determined by the inverse Fourier transformation of $g_i(k_{\perp}^2 + k_x^2)$ with respect to the variable k_x . Their analytical form can be found in ref. [12] for the singlet channel and in ref. [15], for the triplet one. The obvious

notation for the CM and relative coordinates in the x -direction is used in eqs. (6) and (7). Of course, the T_{ij} coefficients depend only on the difference $t = X - X'$ of the CM coordinates. In the perpendicular direction, the total momentum \mathbf{P}_{\perp} and the relative momentum \mathbf{k}_{\perp} are introduced.

Substitution of eqs. (6) and (7) into eq. (3) results in a set of one-dimensional integral equations:

$$G_{ij}(X, X'; E, \mathbf{P}_{\perp}) = T_{ij}(X - X'; E, \mathbf{P}_{\perp}) + \sum_{lm} \int dX_1 dX_2 T_{il}(X - X_1; E, \mathbf{P}_{\perp}) \times \delta B_{lm}(X_1, X_2; E, \mathbf{P}_{\perp}) G_{mj}(X_2, X'; E, \mathbf{P}_{\perp}), \quad (8)$$

where

$$\delta B_{lm} = B_{lm} - B_{lm}^{\text{fr}} \quad (9)$$

is the difference between the convolution B_{lm} of the two-particle propagator A with two form factors g_l, g_m and the analogous convolution B_{lm}^{fr} for the free propagator A^{fr} . The explicit form of B_{lm} is as follows:

$$B_{lm}(X, X'; E, \mathbf{P}_{\perp}) = \sum_{nn'} \int \frac{d\mathbf{k}_{\perp}}{(2\pi)^2} \frac{(1 - n_{\lambda})(1 - n_{\lambda'})}{E - P_{\perp}^2/4m - \varepsilon_n - \varepsilon_{n'} - k_{\perp}^2/m} \times g_{nn'}^l(k_{\perp}^2, X) g_{n'n}^m(k_{\perp}^2, X'). \quad (10)$$

Here we have used a short notation of $\lambda = (n, \mathbf{p}_{\perp})$, $\lambda' = (n', \mathbf{p}'_{\perp})$, $\mathbf{p}_{\perp} = \mathbf{P}_{\perp}/2 + \mathbf{k}_{\perp}$, $\mathbf{p}'_{\perp} = \mathbf{P}_{\perp}/2 - \mathbf{k}_{\perp}$, and $n_{\lambda} = \theta(\mu - \varepsilon_{\lambda})$, where $\varepsilon_{\lambda} = \varepsilon_n + p_{\perp}^2/2m$, and ε_n are the eigenenergies of the one-dimensional Schrödinger equation with the Saxon-Woods potential. The corresponding eigenfunctions $y_n(x)$ (they are chosen to be real) enter the matrix elements of the form factors

$$g_{n,n'}^l(k_{\perp}^2, X) = \int dx g_l(k_{\perp}^2, x) y_n(X+x/2) y_{n'}(X-x/2). \quad (11)$$

It should be noted that the symbolic sum over nn' in eq. (10) actually includes the summation over discrete states and the integration over the continuum spectrum with the standard substitution $\sum_n \rightarrow \int dp/2\pi$.

In the singlet channel, the BG equation for the G -matrix is very similar to the one for the effective pairing interaction [12]. Just as in the latter case, it is convenient to extract the singular δ -form Born term from the complete G -matrix:

$$G = \mathcal{V} + \delta G. \quad (12)$$

The equation for the correlation component δG of the G -matrix can be readily found from eq. (1):

$$\delta G = \mathcal{V}A\mathcal{V} + \mathcal{V}A\delta G. \quad (13)$$

An analogous extraction of the Born term should be made also for the T -matrix:

$$T = \mathcal{V} + \delta T. \quad (14)$$

As a result, the renormalized eq. (3) yields

$$\delta G = \mathcal{F} + T(A - A^{\text{fr}})\delta G, \quad (15)$$

where the inhomogeneous term is

$$\mathcal{F} = \delta T + T(A - A^{\text{fr}})\mathcal{V}. \quad (16)$$

The explicit transformation of eqs. (15), (16) to a form similar to eq. (8) is quite obvious. A simplification of the numerical procedure for solving eq. (15) in the slab system under consideration can be made using the parity conservation which follows from the symmetry of the Hamiltonian under the axis reflection $x \rightarrow -x$. As a result, the eigenfunctions y_n can be divided into even, y_n^+ , and odd, y_n^- , functions. Then the two-particle propagator in the above equations splits into the sum

$$A = A^+ + A^- \quad (17)$$

of the even and odd components. The first one, A^+ , originates from the terms of the sum in eq. (10) containing states (λ, λ') with the same parity, and the second one, A^- , from those with opposite parity. So long as the NN potential \mathcal{V} does conserve the parity, the propagators A^+ and A^- do not mix in the BG equation. Therefore, the correlation part of the G -matrix is also a sum of the even and odd components,

$$\delta G = \delta G^+ + \delta G^-, \quad (18)$$

which obey the separated equations

$$\delta G^\pi = \mathcal{V}A^\pi\mathcal{V} + \mathcal{V}A^\pi\delta G^\pi, \quad (19)$$

π is the parity.

It is obvious that the integral equation (19) can be reduced to the form containing positive x -values only which simplifies the calculations. This equation should be solved for both values of π separately, then the complete G -matrix could be found from eqs. (12),(18).

All the above general equations remain valid for the triplet channel $S = 1$. The main change occurs in the definition of the convolution integral in eq. (10). For the triplet channel it has the form

$$\begin{aligned} B_{lm}^{S=1}(X, X'; E, \mathbf{P}_\perp) = & \sum_{nn'} \int \frac{d\mathbf{k}_\perp}{(2\pi)^2} \frac{(1 - n_\lambda)(1 - n_{\lambda'})}{E - P_\perp^2/4m - \varepsilon_n - \varepsilon_{n'} - k_\perp^2/m} \\ & \times \left(g_{nn'}^{(0)l}(k_\perp^2, X) g_{n'n}^{(0)m}(k_\perp^2, X') \right. \\ & \left. + g_{nn'}^{(2)l}(k_\perp^2, X) g_{n'n}^{(2)m}(k_\perp^2, X') \right). \end{aligned} \quad (20)$$

It should be noted also that all multipole expansions of eqs. (6) and (7) take the form of 2×2 matrices. For example, let us write down the components of the G -matrix in the explicit form

$$\begin{aligned} G^{LL'}(k_\perp^2, k_\perp'^2, \mathbf{P}_\perp; x_1, x_2, x_3, x_4; E) = & \\ \sum_{ij} G_{ij}(X, X'; E, \mathbf{P}_\perp) g_i^{(L)}(k_\perp^2, x) g_j^{(L')}(k_\perp'^2, x'), \end{aligned} \quad (21)$$

where L, L' are equal to 0 or 2.

3 Choice of the model space and the local potential approximation

The main computational problem of solving the BG equation for the slab system is connected with the calculation of the propagators, eqs. (10) and (20). The reason for introducing the model space $S_0(E_0)$, by splitting the complete Hilbert space $S = S_0 + S'$ and using the LPA in the complementary space S' , is as follows. The subspace $S_0(E_0)$ contains all the two-particle states (λ, λ') with both single-particle energies $\varepsilon_\lambda, \varepsilon_{\lambda'}$ smaller than E_0^2 . In the complementary subspace, $S'(E_0)$, one of these energies or both of them are large, $\max(\varepsilon_\lambda, \varepsilon_{\lambda'}) > E_0$. In the model space, the contribution of each individual state (λ, λ') ³ to the sum of eq. (10) or eq. (20) is strengthened, in comparison with the analogous one in the complementary space, due to a small value of the energy denominator. Such contributions produce the long-range terms of the BG propagator A [15] and must be calculated in a direct way. On the contrary, in the complementary subspace no individual state (λ, λ') is important and only wide intervals of the integration over k_\perp significantly contribute to A . The corresponding term of the BG propagator is sharply peaked and is mainly determined by the local properties of the system [15]. Therefore it is natural to use for it some kind of local approximation. For the problem under consideration, it seems to be more natural to use LPA rather than LDA because the BG propagator in the vicinity of the point X is determined directly by the potential well $V(X)$ but not by the density, $\rho(X)$. At the same time, in the surface region there is no simple local relation between $\rho(X)$ and $V(X)$.

The splitting of the Hilbert space $S = S_0 + S'$ results in the representation of the BG propagator as a sum of two terms:

$$A = A_0 + A', \quad (22)$$

where A_0 contains the states (λ, λ') which belong to the model space, A' including the rest. In accordance with the above considerations, we calculate the model space propagator A_0 explicitly, but use LPA for the remaining term A' . Obviously, the accuracy of LPA becomes higher with the model space S_0 becoming wider. We consider LPA to be good at some value of E_0 if the results for the G -matrix do not practically change with additional increase of E_0 .

The LPA procedure, in principle, is the same for both the channels under consideration and it is very close to the one for the pairing problem [12], the latter corresponding to the choice $E_0 = 0$. Namely, for fixed values of the CM coordinates X_{12}, X_{34} , the convolution integral in eq. (10) for $S = 0$ (or eq. (20), for $S = 1$) is replaced by the corresponding integral for nuclear matter put in the constant potential well $V_0 = V(X)$, where $X = (X_{12} + X_{34})/2$, which depends on the difference of the CM coordinates

² In fact, the difference $\varepsilon_\lambda - \mu$ is small. Just such differences enter the denominator of eq. (10) at $E = 2\mu$.

³ The ‘‘individual’’ state means the fixed value of n, n' and a small interval of integration over k_\perp .

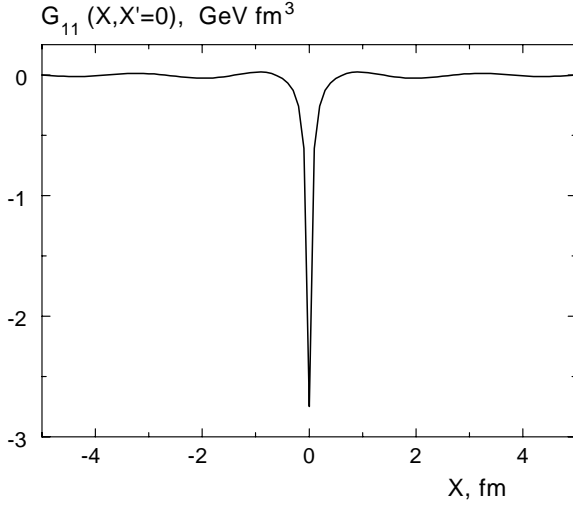


Fig. 1. The profile function $\delta G_{11}(X, X' = 0)$ in the singlet channel for $E_0 = 20$ MeV.

$$t = X_{12} - X_{34}:$$

$$B_{lm}^{\text{LPA}}(X_{12}, X_{34}; E, \mathbf{P}_\perp) = B_{lm}^{\text{inf}}(V[X], t; E, \mathbf{P}_\perp). \quad (23)$$

In practice, for a fixed value of the chemical potential μ and the cut-off energy E_0 and a given set of the potential depths V_n , we calculate a basic set $B_{lm}^{\text{inf}}([V_n], t; E = 2\mu)$ of nuclear matter propagators. In fact, we used a sequence of $V_n = \delta V \cdot (n - 1)$ with the step $\delta V = 2$ MeV. At a fixed coordinate set X_k , the elements of the LPA propagator matrix $B_{lm}^{\text{LPA}}(X_i, X_k)$ are found as follows. First, we find the potential depth $V(X_0 = (X_i + X_k)/2)$. Then, for a fixed value of $t = |X_i - X_k|$, the LPA propagator is found by a linear extrapolation of two neighboring values of $B_{lm}^{\text{inf}}([V_n], t; E)$, $B_{lm}^{\text{inf}}([V_{n+1}], t; E)$, under the condition that the inequality $V_n < V(X_0) < V_{n+1}$ is satisfied. The convolution integral B_{lm}^{fr} for the free propagator A^{fr} , by definition, coincides with $B_{lm}^{\text{inf}}([V_1 = 0], t; E)$. Details can be found in refs. [12, 15].

4 Validity of the LPA for the singlet channel

Up to now, we dealt with the general form of the BG equation for the slab system containing the total perpendicular momentum P_\perp as a parameter. As it was discussed above, the “dangerous” terms of the propagator (or of the convolution integrals in eq. (10)) which belong to the model space and should be considered explicitly, occur due to the small value of the corresponding denominators in the sum of eq. (10). It is obvious that they become more dangerous if the value of P_\perp becomes smaller. Hence the case of $P_\perp = 0$ is most crucial for validity of LPA. Therefore, we consider just this particular “bad” case for the LPA. Then, we only focus on $\mu = -8$ MeV which is a chemical potential typical of stable nuclei. Thus, we put in all the above equations $P_\perp = 0, E = -16$ MeV (omitted for brevity from now on).

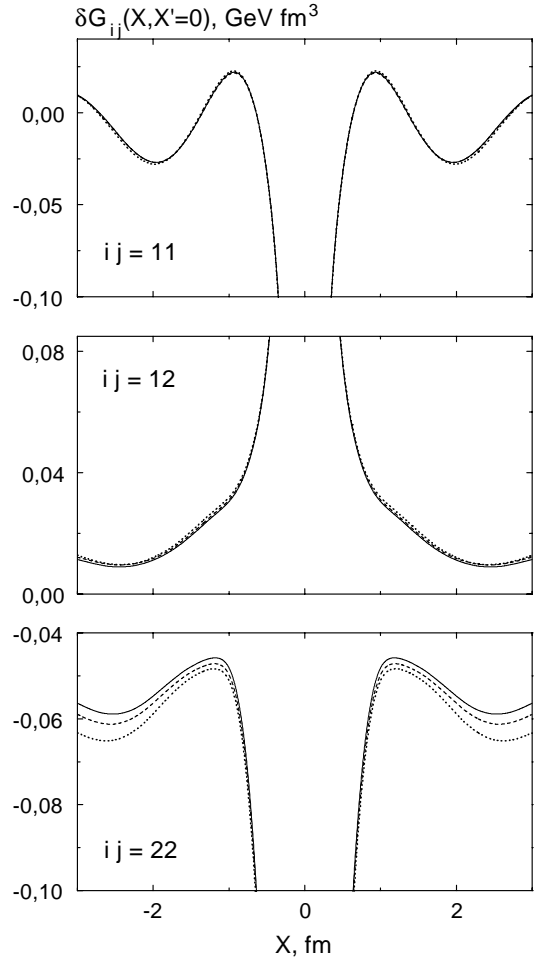


Fig. 2. The profile functions $\delta G_{ij}(X, X' = 0)$ in the singlet channel for $E_0 = 0$ (dotted lines), $E_0 = 10$ MeV (dashed lines), and $E_0 = 20$ MeV (solid lines).

As discussed above, the BG equation for the correlation part of the G -matrix, eq. (13), has a fixed parity π . Therefore, we deal with eq. (19) with fixed π which is defined only for positive x . After finding the convolution integrals in eq. (10) and those for the free propagator A^{fr} , the kernel of eq. (15) and the inhomogeneous term, eq. (16), are derived by direct integration. Then one obtains a set of integral equations for *six* independent components of $\delta G_{ij}^\pi(X, X')$ (similar to eq. (8)) which can be solved numerically [12], [15]. Finally, we find the total correlation δG -matrix, eq. (18), with components $\delta G_{ij}(X, X')$ or, from eq. (12), the complete G -matrix with components $G_{ij}(X, X')$. They differ by a trivial δ -function term

$$\delta G_{ij}(X, X') = G_{ij}(X, X') - \lambda_{ij} \delta(X - X'). \quad (24)$$

The extraction of the latter makes the quantity under consideration more convenient for analysis and graphical representation. Therefore, as a rule, we will deal only with the correlation part of the G -matrix, and not with the complete one. One additional remark should be also made before discussing the results. Following ref. [12], we

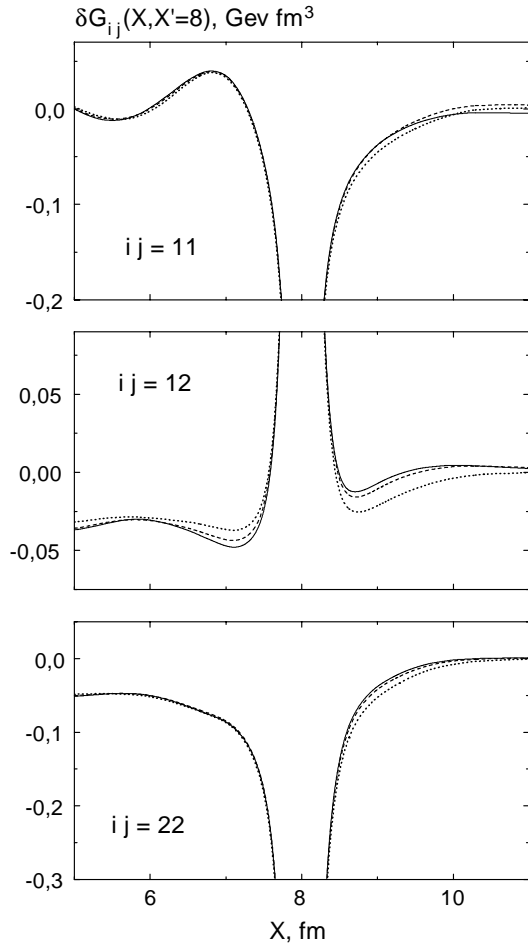


Fig. 3. The profile functions $\delta G_{ij}(X, X' = 8)$ in the singlet channel for $E_0 = 0$ (dotted lines), $E_0 = 10$ MeV (dashed lines), and $E_0 = 20$ MeV (solid lines).

change the original normalization [17,18] of the expansion in eq. (4) so that $g_i(0) = 1$. In this case, the absolute values of the λ_{ij} -coefficients give direct information on the strength of the corresponding terms of the force. Their values (in $\text{MeV} \cdot \text{fm}^3$) are as follows: $\lambda_{11} = -3.659 \cdot 10^3$, $\lambda_{12} = 2.169 \cdot 10^3$, $\lambda_{22} = -1.485 \cdot 10^3$ and $\lambda_{13} = -2.36 \cdot 10^1$, $\lambda_{23} = 5.76 \cdot 10^1$, $\lambda_{33} = 1.72 \cdot 10^1$. The strengths of all the components containing only the indices $i = 1, 2$ are much stronger (by two orders of magnitude) than those with the index $i = 3$. Therefore, the latter are important only for large momenta which come virtually to the BG equation or the Lippman-Schwinger one⁴. If one analyzes the matrix elements of the G -matrix over the nuclear wave functions, the typical momenta $k \simeq k_F$ appear for which the contribution of the small components is negligible. Therefore, as a rule, we concentrate on the “big” components in a qualitative analysis. Of course, in the calculations all the terms λ_{ik} are taken into account.

⁴ Their contribution at high momenta k turns out to be noticeable because the form factor $g_3(k)$ is growing with k , whereas $g_1(k)$ and $g_2(k)$ are vanishing with k rapidly.

We made a series of calculations of the G -matrix for several values of the cut-off energy $E_0 = 0, 10, 20$ MeV to analyze the dependence of the results on this parameter. To present the results we draw the profile functions $\delta G_{ij}(X, X' = X_0)$ of the correlation term of the G -matrix at several values of X_0 and the zero moment of the G -matrix:

$$\bar{G}_{ij}(X) = \int_{-\infty}^{\infty} dt G_{ij}(X, X+t). \quad (25)$$

A typical example of the profile function of $\delta G_{11}(X, X' = 0)$ is shown in fig. 1 for the case of the model space with the cut-off energy $E_0 = 0$. It has a sharp peak at the point $X = X'$. In such a scale, similar curves for $E_0 = 10$ and 20 MeV are distinguishable from that for $E_0 = 0$ only after magnification. Such magnified profile functions for large components with $ij = 11, 12, 22$ are shown in fig. 2, for $X' = 0$, and in fig. 3, for $X' = 8$ fm. It is easily seen that already the difference between the curves for $E_0 = 0$ and $E_0 = 10$ MeV is rather small. As to that for $E_0 = 10$ MeV and $E_0 = 20$ MeV, it looks negligible.

To analyze the dependence of the G -matrix on E_0 in a more quantitative way, it is worth to consider the zero moments, eq. (25), at different values of E_0 . They are shown in fig. 4 for the same large components and, as an example, for one small component, $ij = 13$. One sees that a difference, at a level of a few percent, exists between the curves for $E_0 = 0$ and $E_0 = 10$ MeV and again the additional increase of E_0 from 10 MeV to 20 MeV does not practically influence the results. This is true not only for big components, but also for small ones.

Finally, we calculated the “Fermi-averaged” G -matrix in the 1S -channel:

$$\langle G_F \rangle_{S=0}(X) = \sum_{ij} \bar{G}_{ij}(X) g_i(k_F^2(X)) g_j(k_F^2(X)), \quad (26)$$

where we have introduced the local Fermi momentum as $k_F(X) = \sqrt{2m(\mu - V(X))}$ at $\mu - V(X) > 0$ and which otherwise takes zero value. Such an average is needed to calculate the Landau-Migdal amplitude in terms of the G -matrix [15]. To this respect, one remark should be made. Though the profile functions $G_{ij}(X, X')$ are strongly peaked at the point $X = X'$, the long range “tails”, which are hardly seen “by eyes” in fig. 1, also contribute to the zero moment, eq. (25)⁵. These terms of the G -matrix appear due to states entering the model space and their contribution to the integral (25) was analyzed in [15] for the case of $E_0 = 0$. When one deals with the the Landau-Migdal amplitude which is supposed to be a short-range coordinate function it is natural to cut these tails. In ref. [15] a recipe was suggested to use the Fermi averaged G -matrix, eq. (26), with the zero moments “with cut-off” which are defined by the integral appearing in the eq. (25), but with limits of $|t| < t_c$, $t_c = 3$ fm. Of course, for the validity of LPA it is not important what kind of

⁵ This contribution depends on ij and is, as a rule, not greater than 10–20%.

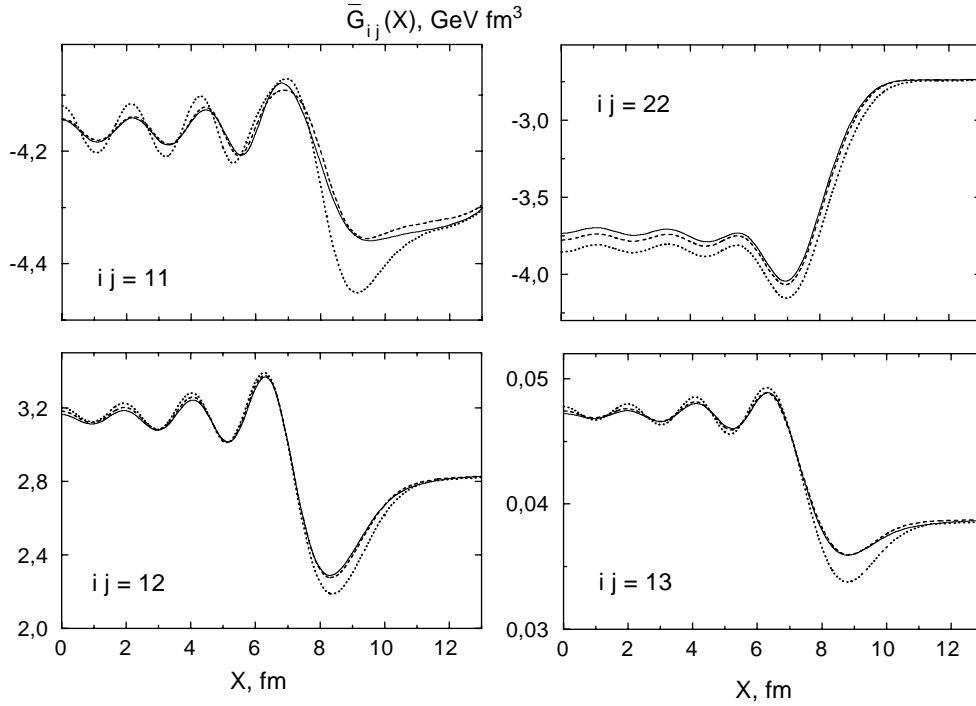


Fig. 4. The zero moments $\bar{G}_{ij}(X)$ in the singlet channel for $E_0 = 0$ (dotted lines), $E_0 = 10$ MeV (dashed lines), and $E_0 = 20$ MeV (solid lines).

zero moment is used in eq. (26). However, we use here the same recipe for the Fermi averaged G -matrix as in ref. [15] because it is more physical. This quantity is shown in fig. 5 for the same three values of E_0 together with the analogous average value of the free off-shell T -matrix:

$$\langle T_F \rangle_{S=0}(X) = \sum_{ij} \bar{T}_{ij}(E=2\mu) g_i(k_F^2(X)) g_j(k_F^2(X)), \quad (27)$$

where the zero moments \bar{T}_{ij} of the T -matrix are defined in the same way as in eq. (25). In this case, the introduction of the cut-off with $t_c = 3$ fm does not practically change the integral. Of course, it is X -independent.

Again, the difference between the Fermi-averaged G -matrix for $E_0 = 10$ MeV and that for $E_0 = 20$ MeV is negligible. Their deviation from the one corresponding to $E_0 = 0$ is also very small everywhere except in the surface region. It should be noted that the difference between the average G -matrix and T -matrix is rather small. A similar property was found previously [13,14] for the effective pairing interaction in the 1S -channel.

Analysis of figs. 2-5 leads us to the conclusion that for the singlet channel $S = 0$ the LPA works pretty well for $E_0 = 10$ – 20 MeV. Moreover, within the accuracy of a few percent, it is also valid for $E_0 = 0$. The latter agrees with the analysis of ref. [12], where the LPA was introduced for the pairing problem in the 1S -channel.

5 Validity of the LPA for the triplet channel

In general, the calculation scheme for the triplet $^3S + ^3D$ channel is very similar to that for the singlet one, though

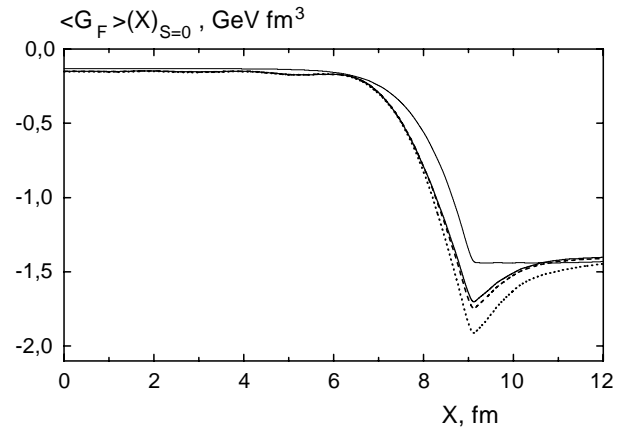


Fig. 5. The Fermi-averaged G -matrix in the singlet channel $\langle G_F \rangle_{S=0}(X)$ for $E_0 = 0$ (dotted line), $E_0 = 10$ MeV (dashed line), and $E_0 = 20$ MeV (solid line) and the Fermi-averaged T -matrix (thin solid line).

the calculations become more cumbersome in this case. Indeed, first, we have to face *ten* independent components $G_{ij}(X, X')$ and *ten* integral equations (8) for them instead of the *six* of the singlet case. Second, the calculation of the convolution integral of eq. (20) in the triplet channel is also more difficult than that of eq. (10). Therefore, the problem of simplifying these calculations is even more important than in the singlet channel.

Contrarily to the singlet case, now it is difficult to separate the multipole terms into the “large” and “small” ones. Again we changed the original normalization [17]

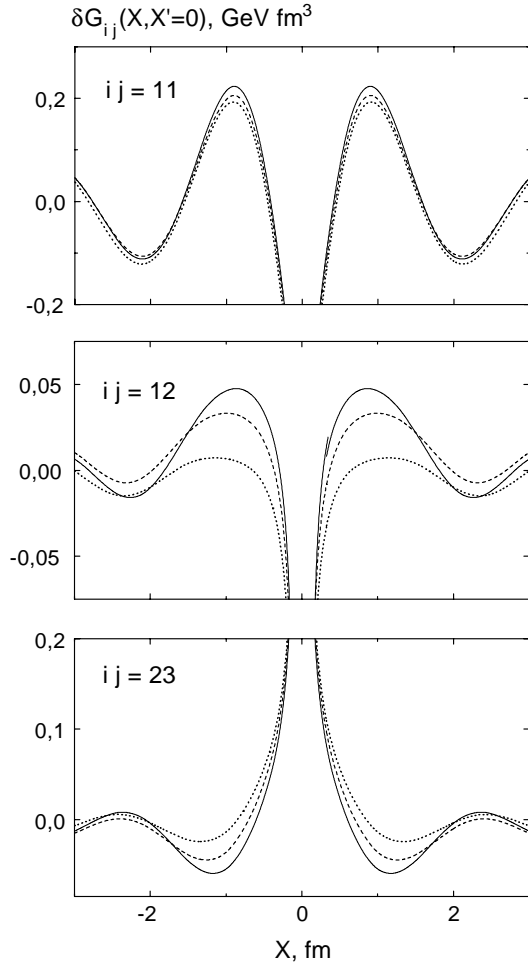


Fig. 6. The same as in fig. 2 for the triplet channel.

of the expansion, eqs. (4),(5), to guarantee the identity $g_i^{L=0}(0) = 1$ (it should be noted that $g_i^{L=2}(0) = 0$). Then the strengths of the corresponding terms of the force (in $\text{MeV}\cdot\text{fm}^3$) are as follows: $\lambda_{11} = -1.618 \times 10^3$, $\lambda_{12} = -1.296 \times 10^3$, $\lambda_{13} = 8.921 \times 10^2$, $\lambda_{14} = 4.271 \times 10^1$, $\lambda_{22} = 7.848 \times 10^2$, $\lambda_{23} = 1.394 \times 10^3$, $\lambda_{24} = -7.860 \times 10^2$, $\lambda_{33} = -7.450 \times 10^2$, $\lambda_{34} = -5.723 \times 10^2$, $\lambda_{44} = 1.865 \times 10^3$. These values show that, though the strengths of different components vary significantly, only one of them, λ_{14} , is smaller by two orders of magnitude as compared to the largest ones. Therefore almost all the terms are important. We take several typical components to illustrate the results.

The profile functions and zero moments are shown in figs. 6-8. One can see that now the results with increasing cut-off energy from $E_0 = 0$ to $E_0 = 10$ MeV change more sizably than in the singlet channel, especially in the surface region. At the same time, the subsequent increase of E_0 up to 20 MeV does not practically influence the G -matrix, the maximum variation being of a few percent. Hence, once more one may conclude that the LPA is sufficiently accurate if the cut-off energy is $E_0 = 10$ -20 MeV. But, contrarily to the singlet case, the accuracy of LPA is rather poor when the model space is limited to $E_0 = 0$,

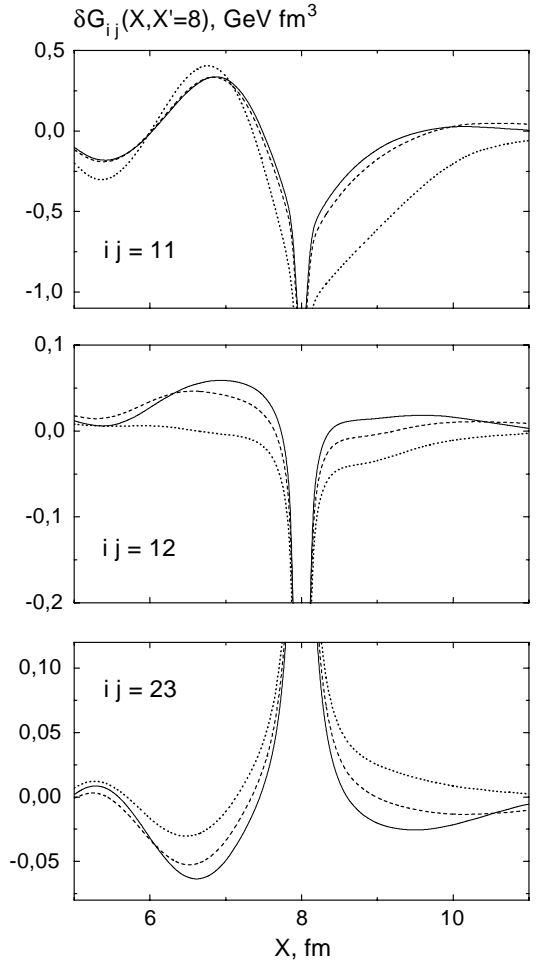


Fig. 7. The same as in fig. 3 for the triplet channel.

since at the surface the G -matrix must tend to the off-shell free T -matrix. But the latter has a virtual pole at small energy. It is then clear that an accurate account of the contribution of the single-particle states with small positive energies is important for a correct description of this pole behavior. Therefore, these states should be included into the model space S_0 . This does occur if one chooses the cut-off energy $E_0 \geq 10$ MeV, but it does not occur if one takes $E_0 = 0$.

Let us now consider the Fermi averaged G -matrix in the triplet channel, which is a 2×2 matrix in the orbital angular momentum space:

$$\langle G_F \rangle_{S=1}^{LL'}(X) = \sum_{ij} \bar{G}_{ij}^{S=1}(X) g_i^{(L)}(k_F^2(X)) g_j^{(L')}(k_F^2(X)), \quad (28)$$

where $L, L' = 0, 2$. Just as in the singlet case, the quantity \bar{G}_{ij} in eq. (28) has the meaning of the zero moment “with cut-off”. The components of this matrix are shown in fig. 9 for all three values of the cut-off energy E_0 . The component $\langle G_F \rangle_{S=1}^{00}$ is significantly larger than those containing $L = 2$, especially at the surface region where the form factors $g_i^{(2)}$ vanish. Again all the components of the Fermi-averaged G -matrix calculated for $E_0 = 10$ MeV co-

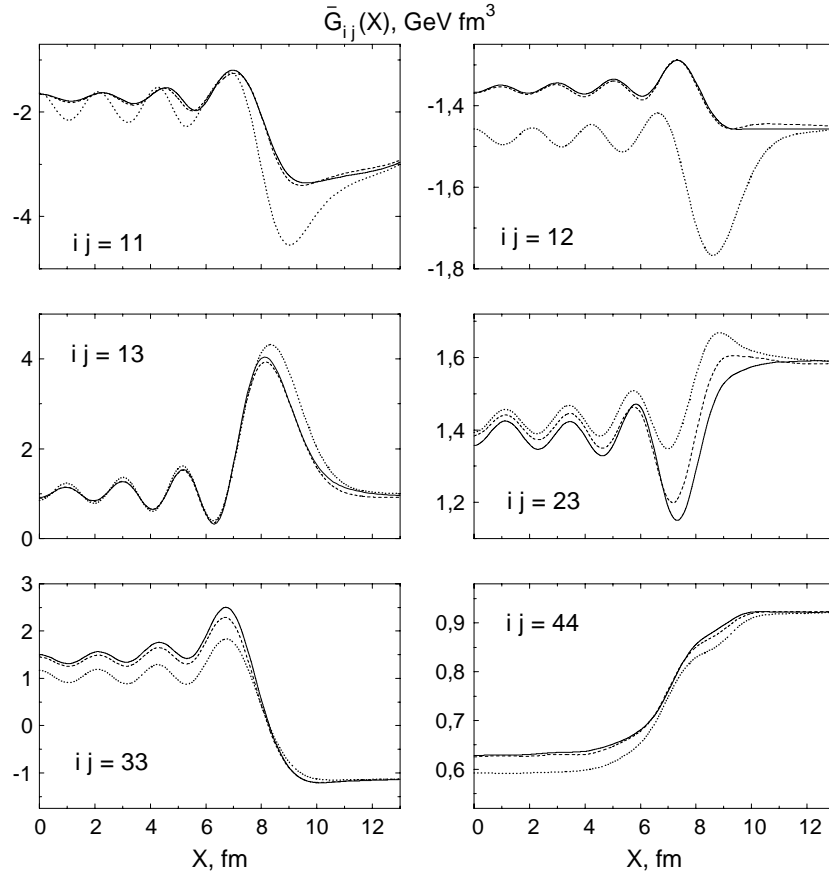


Fig. 8. The same as in fig. 4 for the triplet channel.

incide practically with those for $E_0 = 20$ MeV, though deviations from the $E_0 = 0$ case can be noticeable.

6 A simple model for the scalar-isoscalar Landau-Migdal amplitude in terms of the free T-matrix

In the framework of the Brueckner theory, the Landau-Migdal quasiparticle interaction amplitude is expressed in terms of the G -matrix as follows:

$$F(\mathbf{r}_1, \mathbf{r}_2, \mathbf{r}_3, \mathbf{r}_4) = \frac{1}{\sqrt{Z(\mathbf{r}_1)Z(\mathbf{r}_2)Z(\mathbf{r}_3)Z(\mathbf{r}_4)}} G(\mathbf{r}_1, \mathbf{r}_2, \mathbf{r}_3, \mathbf{r}_4; E = 2\mu), \quad (29)$$

where $Z(\mathbf{r})$ is the renormalization factor of the single-particle Green function.

In the standard notation adopted in the FFS theory, the central part of the Landau-Migdal amplitude reads

$$F = C_0 [f + f' \tau_1 \tau_2 + (g + g' \tau_1 \tau_2) \sigma_1 \sigma_2], \quad (30)$$

where σ and τ are the spin and isospin Pauli matrices. The normalization factor C_0 is the inverse density of states at the Fermi surface: $C_0 = (dn/d\varepsilon_F)^{-1}$. We shall analyze here the zero harmonic f_0 of the scalar-isoscalar component of eq. (30) which is responsible for the central part of

the average nuclear field. In the FFS theory, a strong coordinate dependence of this amplitude was introduced [4] to explain various types of experimental data. In fact, the simplest form of such a dependence, proposed in ref. [4], is

$$f_0(\mathbf{r}) = f_0^{\text{ex}} + (f_0^{\text{in}} - f_0^{\text{ex}}) \frac{\rho(\mathbf{r})}{\rho_0}. \quad (31)$$

Here, $\rho(\mathbf{r})$ is the nuclear density at the point \mathbf{r} , and $\rho_0 = \rho(r = 0)$. It is worth to note that different versions of the interpolation formula for the amplitude $f_0(\mathbf{r})$ exist, but the common feature of all of them is a significant difference between a large negative external constant f_0^{ex} and a small (close to zero) internal one, f_0^{in} .

We shall see now that the typical coordinate dependence of eq. (31) for the scalar-isoscalar Landau-Migdal amplitude can be approximately obtained within the Brueckner approach, eq. (29). As far as the Landau-Migdal amplitude corresponds to the interaction of two quasiparticles at the Fermi surface, the Fermi averaged G -matrices, eqs. (26) and (28), appear in the relation for $f_0(r)$ resulting from eq. (29). Going from a slab to the spherical geometry for a heavy nucleus with a large radius $R \simeq L$, after simple spin-isospin algebra, we find

$$f_0(r, E) = \frac{3}{16} Z^2(r) (\gamma_0(r, E) + \gamma_1(r, E)), \quad (32)$$

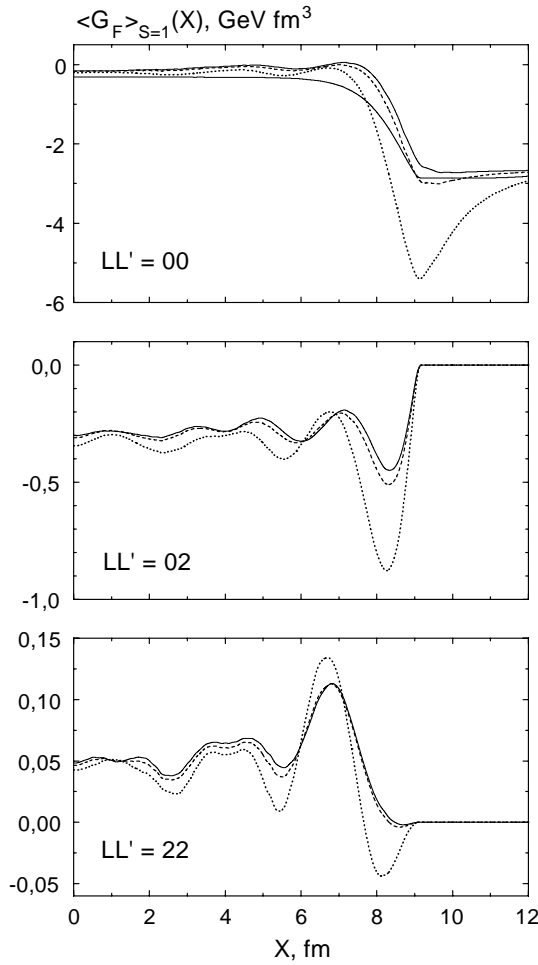


Fig. 9. The same as in fig. 5 for the triplet channel.

where we have introduced the dimensionless Fermi-averaged G -matrices

$$\gamma_{0,1}(X, E) = \frac{1}{C_0} \langle G_F^{S=0,1} \rangle(X, E). \quad (33)$$

Only the main $L = L' = 0$ component is retained in the triplet case.

Up to now, we considered the value of the total perpendicular momentum P_\perp . It can be directly used in eq. (32) only in the asymptotic region where all the particle momenta vanish. Inside the nucleus the Fermi averaging procedure should include integration over P_\perp from 0 to $2k_F$. An accurate method of averaging over P_\perp is not yet developed but we can use the following approximate recipe. Let us consider the surface region $r \simeq R$, where the operator P_\perp^2 can be replaced by the number $P_\perp^2 = \mathcal{L}(\mathcal{L} + 1)/R^2$, \mathcal{L} being the total two-particle orbital angular momentum. The integration over P_\perp corresponds to the summation over all possible values of \mathcal{L} . In a heavy nucleus, the maximum values of the single-particle orbital angular momenta, $l_{\max} = 6-7$, hence we get $\mathcal{L}_{\max} = 12-14$. To estimate the role of non-zero values of P_\perp , we calculated, following the recipe of ref. [15], the G -matrix in both channels at the value $P_\perp^2 = 0.656 \text{ fm}^{-2}$. The latter is obtained

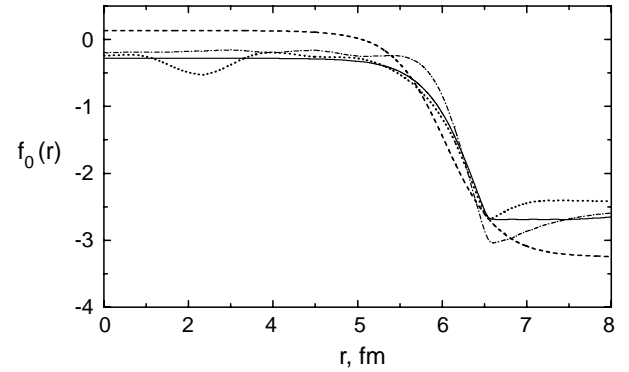


Fig. 10. The microscopic scalar-isoscalar Landau-Migdal amplitude $f_0(X)$ calculated in terms of the G -matrix with zero P_\perp (dash-dotted curve) and non-zero P_\perp (dotted curve) together with that within the semi-microscopic model in terms of the free T -matrix (solid curve). The phenomenological amplitude of the self-consistent FFS theory [6] is shown by the dashed line.

by substituting the average value $\mathcal{L} = 6$ and $R = 8$ fm in the above expression for P_\perp^2 .

In addition to the G -matrix, the formula (32) contains the Z -factor. Calculation of this quantity is beyond the scope of this article and we use for $Z(r)$ the phenomenological ansatz of the self-consistent FFS theory [6]:

$$Z(r) = \frac{2}{1 + \sqrt{1 - 4C_0\alpha_2\rho(r)/\varepsilon_F^0}}, \quad (34)$$

where $\varepsilon_F^0 = (k_F^0)^2/2m$ (the normalization value of the Fermi momentum is $k_F^0 = \pi^2/(mC_0)$), and the dimensionless parameter $\alpha_2 = -0.25$.

The scalar-isoscalar amplitude $f_0(r)$ calculated according to eqs. (32), (34) for zero and non-zero values of P_\perp is shown in fig. 10. They are close to each other in the inner domain and slightly differ at the surface and in the asymptotic region. It is obvious that the function $f_0(r)$ corresponding to $P_\perp = 0$ possesses correct asymptotic behaviour, while the one with non-zero P_\perp should be more correct at the surface and in all the classically allowed region. Therefore, a reasonable recipe consists in matching these two functions at the surface. It turned out that the necessary interpolation can be successfully simulated within a very simple semi-microscopic model in which the amplitude $f_0(r)$ is calculated according to eqs. (32), (34), but substituting the free T -matrix (at $P_\perp = 0$) for the G -matrix. This model amplitude is also drawn in fig. 10. It should be stressed that this quantity is found by a very simple calculation because the T -matrix in the coordinate representation can be easily obtained (see, e.g., [14,15]). For comparison, the phenomenological scalar-isoscalar Landau-Migdal amplitude of the self-consistent FFS theory [6] is also displayed. The model amplitude is in reasonable agreement with the phenomenological one. This simple model for the scalar-isoscalar Landau-Migdal amplitude was recently proposed in ref. [16], but the analysis was based on the calculation of the G -matrix within LPA with the “standard” model space ($E_0 = 0$).

As we have seen above, in this case, the LPA is not sufficiently correct for the triplet channel. Here, we repeated the calculations of ref. [16] for the model space with $E_0 = 10$ MeV where the LPA is quite accurate for both channels. For the scalar-isoscalar amplitude, the results of the advanced calculation of the G -matrix in this paper are imitated by the free T -matrix even more accurately than in ref. [16]. Thus, this analysis justifies the simple model for $f_0(r)$ proposed in ref. [16].

7 Conclusion

The applicability of the LPA has been analyzed for the Brueckner G -matrix. Previously [12] this kind of local approximation proved to be quite accurate for the problem of the microscopic evaluation of the effective pairing interaction in the 1S -channel. The BG equation for a slab of nuclear matter has been solved for the singlet 1S and triplet $^3S + ^3D$ channels using the separable representation [17,18] of the Paris potential. The complete Hilbert space has been split into two domains separated by the energy E_0 . The model subspace $S_0(E_0)$, in which the two-particle BG propagator is calculated explicitly, contains all the two-particle states with both single-particle energies $\varepsilon_\lambda, \varepsilon_{\lambda'} < E_0$. In the complementary subspace, $S'(E_0)$, the LPA for the BG propagator has been used. A qualitative analysis shows that the accuracy of LPA becomes higher with increasing E_0 . It should also be higher for larger values of the perpendicular total momentum P_\perp , therefore we limited ourselves to the most “dangerous” case of $P_\perp = 0$.

For either channel under consideration, a set of calculations of the G -matrix has been made for different values of the cut-off energy E_0 . The LPA has been assumed to be valid starting from the value of E_0 for which the G -matrix does not practically change any longer. An approximate independence of results on the value of E_0 , at a level of a few percents, was found for $E_0 = 10$ –20 MeV for both channels. It should be mentioned that in the singlet channel the accuracy of the LPA is sufficiently high even at $E_0 = 0$, in accordance with ref. [12]. On the contrary, in the triplet channel the LPA is not practically applicable for $E_0 = 0$. A similar analysis could be made also for the channels with $L > 0$. Estimates show that in this case conditions for validity of LPA are even better than those for $L = 0$.

Although we only considered a separable version of the Paris potential only, all the physical reasons for a high accuracy of the LPA remain valid for any realistic NN potential. We believe that the LPA works pretty well in the microscopic description of finite nuclear systems.

We used the obtained G -matrix for justifying a simple microscopic model of the scalar-isoscalar component of the

Landau-Migdal amplitude in terms of the free T -matrix.

In this paper, we limited ourselves to just one value of the chemical potential $\mu = -8$ MeV which is typical of stable nuclei. In principle, for smaller values of μ the analysis should be repeated. However, as some estimates show, even in the drip line vicinity, where $\mu_n \rightarrow 0$ (or $\mu_p \rightarrow 0$) the LPA should be rather good for $E_0 = 10$ –20 MeV in either channel. At the same time, at $E_0 = 0$ it should become inapplicable even in the singlet channel.

This research was partially supported by Grants No. 00-15-96590 and No. 00-02-17319 from the Russian Foundation for Basic Research. The discussions with P. Schuck are highly acknowledged. We shall never forget the sincere interest paid to our work by S.A. Fayans, who has recently passed away.

References

1. V.M. Strutinsky, Nucl. Phys. A **95**, 420 (1967); **122**, 1 (1968).
2. P. Möller, J.R. Nix, W.D. Myers, W.J. Swiatecki, At. Dat. Nucl. Data Tables **59**, 5 (1995).
3. Y. Aboussir, J.M. Pearson, A.K. Dutta, F. Tondeur, At. Dat. Nucl. Data Tables **61**, 127 (1995).
4. A.B. Migdal, *Theory of Finite Fermi Systems and Applications to Atomic Nuclei* (Interscience, New York, 1967).
5. A.B. Migdal, *Theory of Finite Fermi Systems and Applications to Atomic Nuclei*, 2nd edition (Nauka, Moscow, 1983).
6. V.A. Khodel, E.E. Saperstein, Phys. Rep. **92**, 183 (1982).
7. D. Vautherin, D. Brink, Phys. Rev. C **5**, 626 (1972).
8. Z. Patyk *et al.*, Phys. Rev. C **59**, 704 (1999).
9. S.A. Fayans, JETP Lett. **68**, 169 (1998); S.A. Fayans, S.V. Tolokonnikov, E.L. Trykov, D. Zawischa, Nucl. Phys. A **676**, 49 (2000).
10. H.A. Bethe, *Theory of Nuclear Matter* (Mir, Moscow, 1974).
11. P. Ring, P. Schuck, *The Nuclear Many-Body Problem* (Springer, Berlin, 1980).
12. M. Baldo, U. Lombardo, E.E. Saperstein, M.V. Zverev, Nucl. Phys. A **628**, 503 (1998).
13. M. Baldo, U. Lombardo, E.E. Saperstein, M.V. Zverev, Phys. Lett. B **477**, 410 (2000).
14. M. Baldo, U. Lombardo, E.E. Saperstein, M.V. Zverev, Phys. At. Nucl. **63**, 1377 (2000).
15. M. Baldo, U. Lombardo, E.E. Saperstein, M.V. Zverev, Phys. At. Nucl. **64**, 203 (2001).
16. M. Baldo, U. Lombardo, E.E. Saperstein, M.V. Zverev, Phys. At. Nucl. **64**, 509 (2001).
17. J. Haidenbauer, W. Plessas, Phys. Rev. C **30**, 1822 (1984).
18. J. Haidenbauer, W. Plessas, Phys. Rev. C **32**, 1424 (1985).
19. M. Lacombe, B. Loiseaux, J.M. Richard, R. Vinh Mau, J. Côté, D. Pirès, R. de Tourreil, Phys. Rev. C **21**, 861 (1980).